The Radiosensitizing Potential of CC-115, PIK-75 and M3814 DNA-PK Inhibitors for Breast Cancer Targeted Radiotherapy

Dragoș Andrei Niculae *, Radu Marian Șerban, Dana Niculae *, Doina Drăgănescu

Posted Date: 12 May 2026

doi: 10.20944/preprints202605.0803.v1

Keywords: DNA-PKcs; NHEJ; copper-64; breast cancer; combination therapy; radiotherapy; DNA damage

 doi:10.20944/preprints202605.0803.v1

Article

The Radiosensitizing Potential of CC-115, PIK-75 and M3814 DNA-PK Inhibitors for Breast Cancer Targeted Radiotherapy

Dragoș Andrei Niculae [1,2,*], Radu Marian Șerban [2], Dana Niculae [2,*] and Doina Drăgănescu [1]

[1] Faculty of Pharmacy, "Carol Davila" University of Medicine and Pharmacy, 37 Dionisie Lupu Street, 020021 Bucharest, Romania

[2] Horia Hulubei National Institute for Physics and Nuclear Engineering, 30 Reactorului Street, 077125 Magurele, Romania

* Correspondence: dragos-andrei.niculae@drd.umfcd.ro (D.A.N.); dananiculae@nipne.ro (D.N.)

Abstract

NHEJ is one of the preferred DNA-damage repairing mechanisms for human cells, due to its rapid onset and activity throughout the cell cycle. It is, nevertheless, error prone and highly relevant in numerous oncological malignancies. In the recent years, it gained a lot of attention as a target either for cancer treatment or synergetic strategies, as pharmacological- and radio-sensitization approaches. This study evaluated the genotoxicity and radiosensitization potential of three DNA-PK inhibitors (PIK-75, M3814, and CC-115) in breast cancer by comparing MDA-MB-231 (NHEJ reliant) and MCF-7 (NHEJ and HR reliant) cell lines. Cells were preincubated with the DNA-PK inhibitors, using four different concentrations either in monotherapy or in combination with a DNA damage-inducer (doxorubicin or [^{64}Cu]$CuCl_2$). Viability was measured by MTS assays at 24, 48, and 72 h, while the DNA damage by γH2AX and flow cytometry. DNA-PK blockade preferentially sensitized NHEJ-reliant breast cancer cells to doxorubicin and ^{64}Cu effect. Combination treatments generally reduced viability relative to inhibitor's monotherapy, with clearer concentration dependence and stronger effects in MDA-MB-231. In the case of [^{64}Cu]$CuCl_2$ alone, MDA-MB-231 viability was reduced to 70–75% at 24 h, whereas several inhibitor combinations reduced it further; MCF-7 showed weaker or inconsistent potentiation. Delayed cytotoxicity was most obvious at 72 h, showing persistence of unrepaired DNA damage after DNA-PK inhibition. Overall, the results highlight the potential of exploiting repair-pathway dependence to improve targeted radiotherapy in breast cancer.

Keywords: DNA-PKcs; NHEJ; copper-64; breast cancer; combination therapy; radiotherapy; DNA damage

1. Introduction

A critical DNA double-strand break (DSB) repair pathway that operates throughout the cell cycle in order to ensure the genomic stability of the cells is the non-homologous end joining (NHEJ) [1,2]. This complex detection and repairing mechanism is capable of repairing DSBs without the need of a homologous template, which makes it a rapid response mechanism when compared to homologous recombination (HR) [3]. Still, the fast response, critical parameter to increase survivability, can make this mechanism prone to errors [1,4].

DNA-dependent protein kinase (DNA-PK) complex is essential for the function of NHEJ, involved in the recruitment and activation of DNA repair factors, such as Artemis, XRCC4, and DNA ligase IV [5–7].

As such, the NHEJ, on which certain cancers types have been proven to relay on for fast DSBs repairmen, became a target for therapeutic approaches [8]. Using different inhibitors to interfere with the activation of the repair mechanism can make cancer cells more vulnerable to chemical and

 doi:10.20944/preprints202605.0803.v1

radiological treatments [9]. Studies have indicated that the presence of DNA-PK inhibitors in cancer cells prior to exposure to radiation can enhance the efficiency of the treatment, or allow the usage of a lower dose that can still have the desired effect [10].

Clinical studies aim to establish a combination therapeutic approach in cancer treatment, by determining how to best exploit the different DNA repair capacities among tumor subtypes, significantly increase the radiosensitivity of cancer cells, while avoiding impacting the healthy tissues, and the technological transfer from preclinical studies to applied clinical therapies [11–14].

PIK-75 is a very potent PI3k and DNA-PK inhibitor [15,16], showing good selectivity for p110α isoform, with IC50s of 2 nM for DNA-PK, and 5.8 nM, 1300 nM, 76 nM and 510 nM for p110α, -β, --γ, and -δ respectively. It acts as a noncompetitive inhibitor with ATP and competitive with PI substrate. Its strong NHEJ inhibition has been shown in multiple studies in nonasthmatic airway smooth muscle (ASM) cells, asthmatic ASM cells, and lung fibroblasts [17], small-cell lung cancer (SCLC) [18], medulloblastoma [19], acute myeloid leukemia (AML) [20], glioblastoma [21], mantle cell lymphoma [13] and was even formulated as HDL-mimetic nanoparticles [16]. PIK-75 has been investigated *in-vivo* as well, showing a reduction in cell invasion in ErbB3WT breast tumor models [22].

M3814 is a specific anti-DNA-PK ligand, with IC50 of 3 nM, that was shown *in-vitro* to strongly block DNA-PK catalytic activity and sensitize cancer cell lines to ionizing radiation (IR) and pharmacological DSB-inducing agents, via rendering the NHEJ pathway incapable of resolving complex DSBs, which leads to an increased number of them and, finally, promoting apoptosis [23]. M3814 was administered orally to two xenograft bearing mice, on a 6-week fractionated radiation schedule, and it potently bolster the radio-therapy efficiency, even leading to complete tumour regression using non-toxic dose regimens [23].

CC-115 is a potent, multi-pathway inhibitor that strongly blocks DNA-PK (0.013 μM), mTOR (0.021 μM) and PI3K (0.852 μM) [24], rendering the targeted cell incapable of critical DNA-damage repair. It was shown to inhibit DNA damage repair in CLL cell lines and induce caspase-dependent cell death path. It was shown to repert CD40-induced chemoresistance, while also blocking cell proliferation [25]. The compound was also tested *in-vivo* in CLL patients, where it showed a decrease in lymphadenopathy. It was shown to cross the blood-brain barrier (BBB) in glioblastoma models, and even allowing one patient to achieve complete remission of endometrial carcinoma for over 4 years [26]. When combined with enzalutamide for metastatic castration-resistant prostate cancer it shown an additional reduction in prostate-specific antigen (PSA) levels [27]. Another important trait is the very good bioavailability of 53, 76 and 100% in mice, rats and respectively dogs, displaying a good pharmacokinetic profile [24].

In this study we investigated the effects those DNA-PK inhibitor have on the cells incubated following exposure to different DNA damaging stress factors. Using initially doxorubicin [28] solutions to induce DNA DSB in order to assess the genotoxic effects the inhibitors would have, and establishing adequate work concentration for each inhibitor. We then studied the radiosensitization effects of the inhibitors by exposure to the emissions of copper-64 radioisotope [29,30].

The study aims to characterize the genotoxic and radiosensitization effects of the selected DNA-PK inhibitors on two breast cancer cell lines, one that relies on the NHEJ pathway in response to DSB, and one NHEJ independent [31].

2. Results

For the first experiment, MDA-MB-231 and MCF-7 cell lines were exposed to 4 different concentrations of DNA-PK inhibitors and the cytotoxic effect was compared to doxorubicin (Figure 1). The inhibitors alone had an impact on the viability of MDA-MB-231 cells, effect that is clearly correlated with the concentration for PIK-75 and CC-115. Nevertheless, the impact of the inhibitors is lower than that of doxorubicin, which indicates that the inhibitors used at these concentrations were better tolerated than the already established pharmacological DSB inducer.

 doi:10.20944/preprints202605.0803.v1

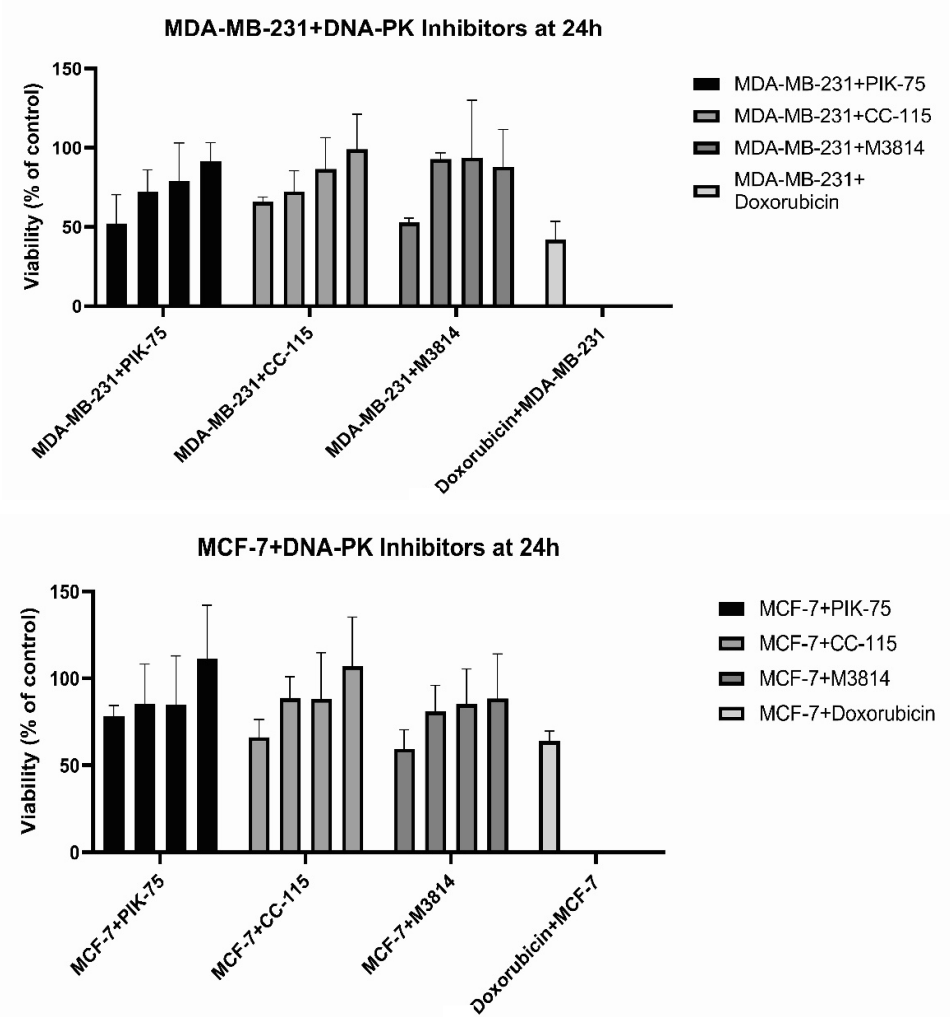

Figure 1. Effect of single therapy of DNA-PK Inhibitors on MDA-MB-231 and MCF-7 normalized to the controls.

For the second experiment, the cell lines were exposed to a combination therapy which consisted of the 4 concentrations of DNA-PK inhibitors with doxorubicin (Figure 2). The cell viability further dropped compared to either the inhibitor or the doxorubicin alone. For MCF-7 cell line we noticed a lower degree of differentiation between the concentrations. Nevertheless, even in this case cells we could see a synergetic effect when doxorubicin was combined with the DNA-PK inhibitors. In the case of MDA-MB-231 cell line, the impact was clearly higher, while the concentration-effect trend was clearer. PIK-75, the most potent inhibitor selected, showed a clear concentration dependent impact on cells' viability.

 doi:10.20944/preprints202605.0803.v1

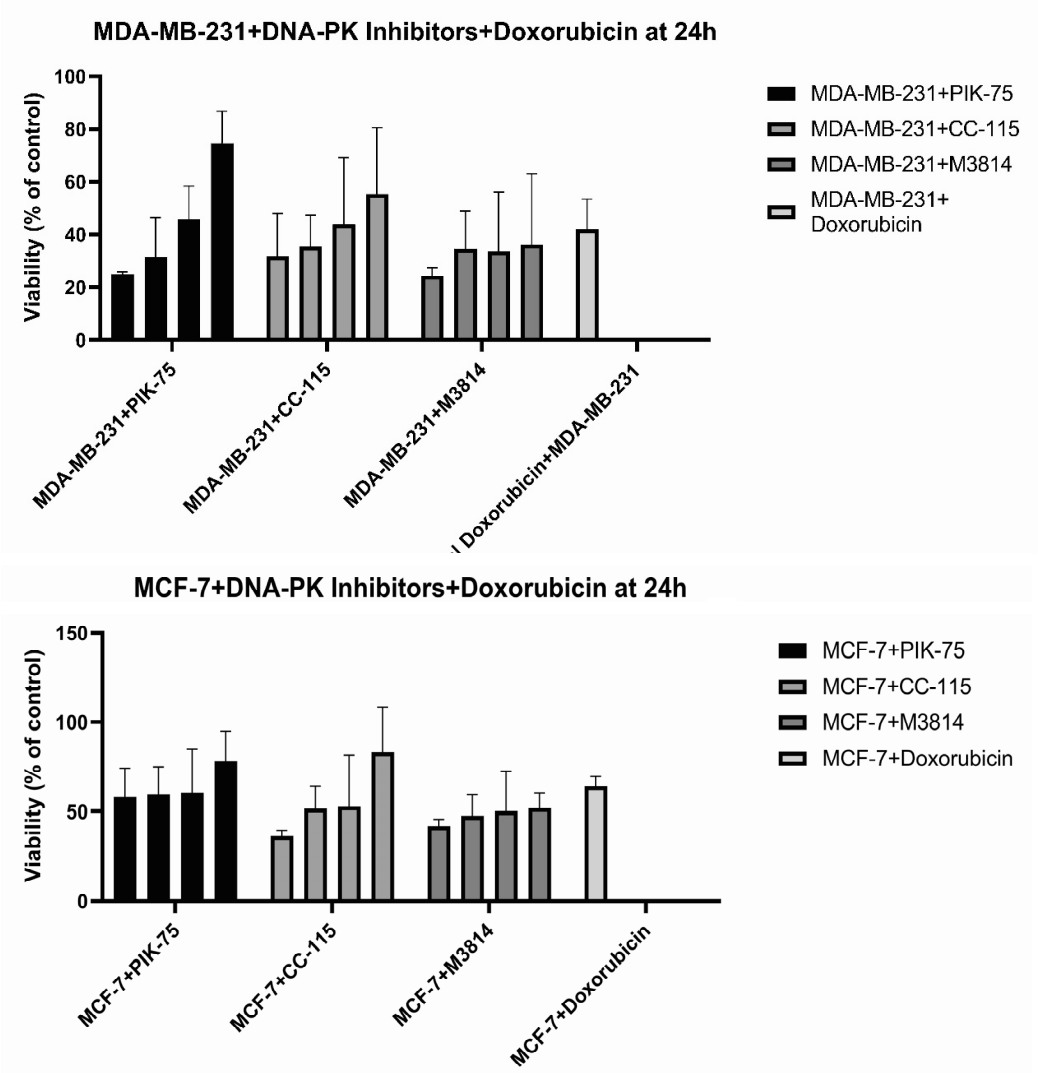

Figure 2. Effect of combination therapy, Doxorubicin + DNA-PK inhibitors, on MDA-MB-231 and MCF-7, normalized to the controls. The last column shows the doxorubicin monotherapy.

For the third part of the experiment, the cell lines were subjected to a combination therapy of [^{64}Cu]$CuCl_2$ and DNA-PK Inhibitors, using the 4 different concentration of inhibitors, same as before (Figure 3). A clear concentration dependent impact was observed for MDA-MB-231 when exposed to PIK-75, as in the case of the other two DNA-PK inhibitors differences appear between concentrations, especially for C1 and C4, while the C2 and C3 show similar outcomes. For MCF-7, the presence of DNA-PK inhibition could stimulate the cellular metabolism, no clear correlation between concentration and effect was observed, and the inhibition was comparative to [^{64}Cu]$CuCl_2$ monotherapy, which indicates that there was no specific targeting effect.

 doi:10.20944/preprints202605.0803.v1

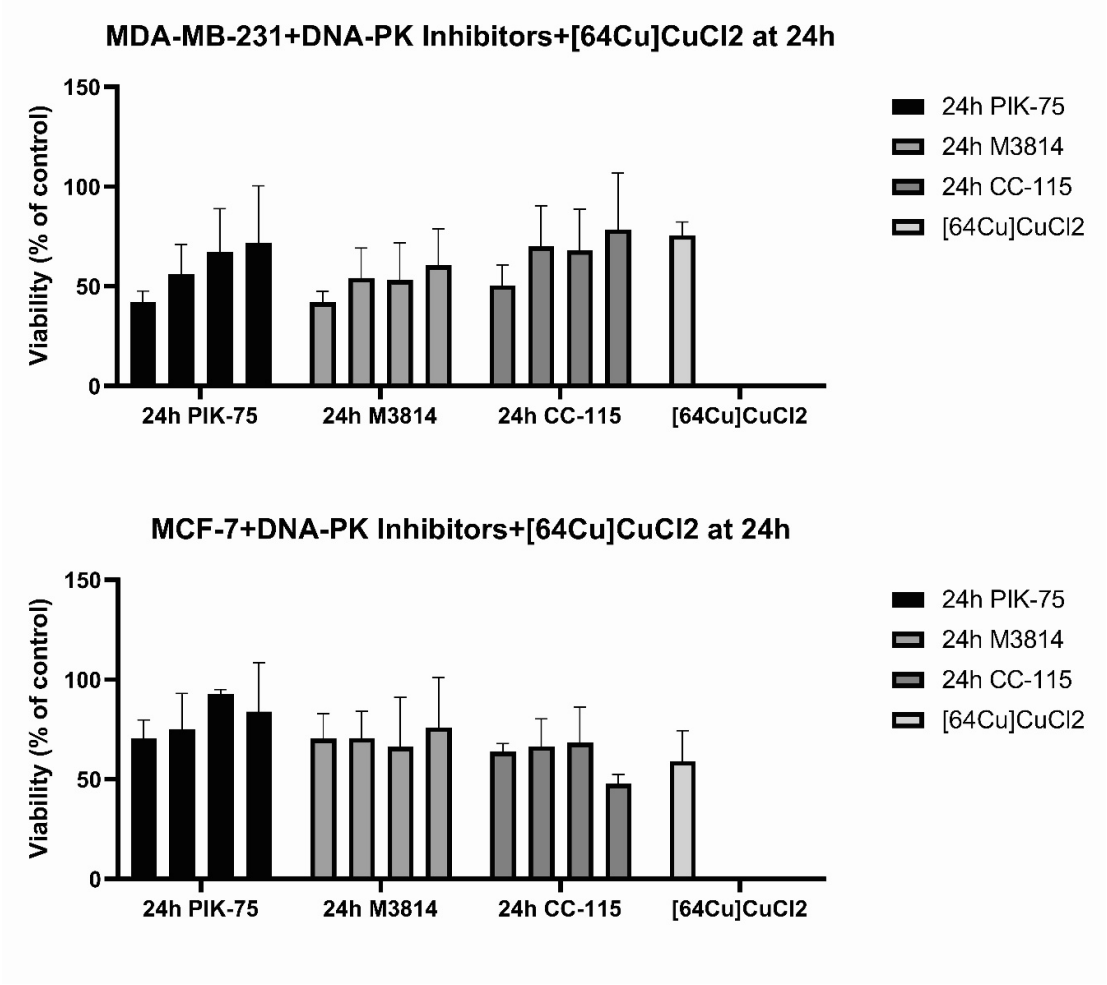

Figure 3. Effect of combination therapy, [^{64}Cu]$CuCl_2$ + DNA-PK inhibitors, on MDA-MB-231 and MCF-7, normalized to the controls; The last column shows the effect of [^{64}Cu]$CuCl_2$ monotherapy.

All experiments included three time-points, 24, 48 and 72 hours, in order to better understand the manner in which the cells adapt to the inhibitor's blockade. DNA-PK inhibitors' C1 was selected for evaluation over all time-points due to its best radiosensitization effect (Figure 4).

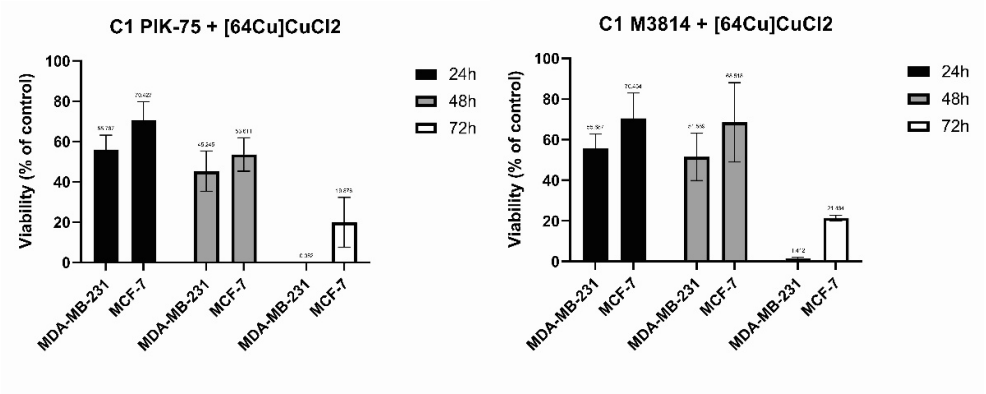

(a) (b)

 doi:10.20944/preprints202605.0803.v1

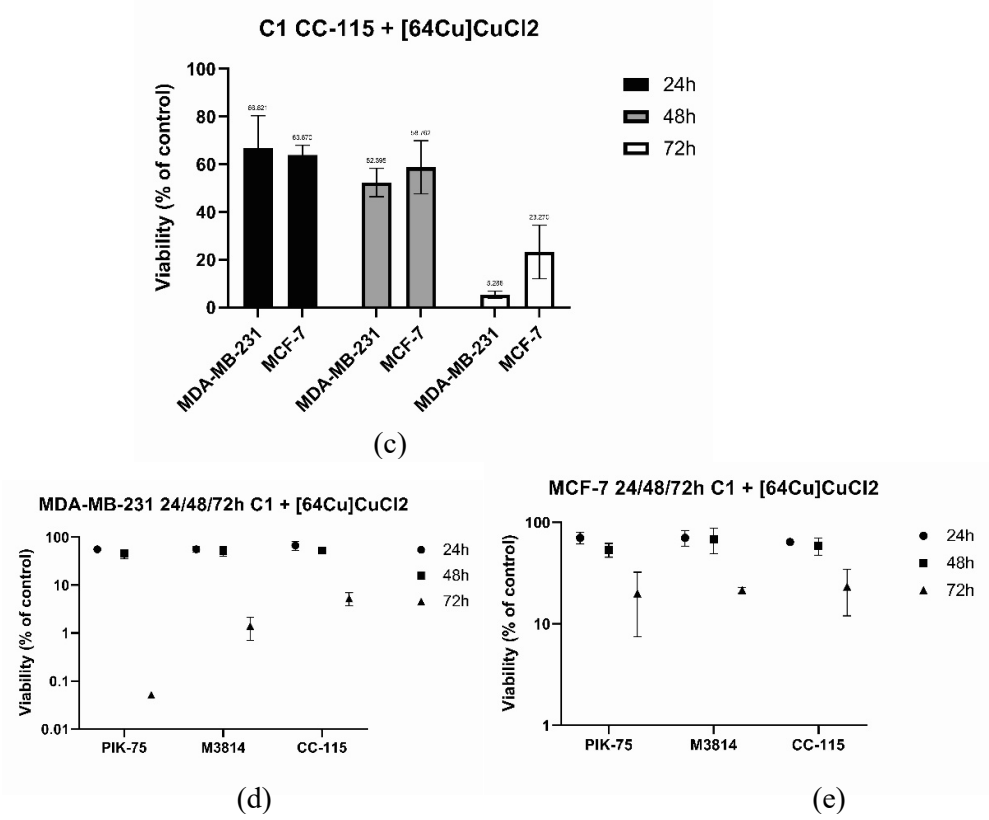

Figure 4. (a). Comparison of the PIK-75 + [^{64}Cu]CuCl$_2$ effect between cell; (b). Comparison of the M3814 + [^{64}Cu]CuCl$_2$ effect between cell lines; (c). Comparison of the CC-115 + [^{64}Cu]CuCl$_2$ effect between cell lines; (d). Logarithmic scale showing the dose-effect curve of the DNA-PK inhibitors + [^{64}Cu]CuCl$_2$ in MDA-MB-231 cell line; (e). Logarithmic scale showing the dose-effect curve of the DNA-PK inhibitors + [^{64}Cu]CuCl$_2$ in MCF-7 cell line; The logarithmic scale was used to show, where possible, the error bars that are not visible in the linear scale;.

We used the γH2AX assay to assess the level of DNA damage induced in the breast cancer cell lines post incubation with the DNA-PK inhibitors, either alone or in combination with doxorubicin. We analyzed γH2AX foci levels following a 4 h of incubation of the two cell lines with the second highest concentration of CC-115 and PIK-75, both with and without the presence of doxorubicin. Results are presented in the Figure 5.

For MCF-7, in the presence of doxorubicin, the γH2AX signal increases, the clearest increase was observed for PIK-75 in combination with doxorubicin. For the MDA-MB-231 cell-lines, both in the doxorubicin and the control, we noticed an increase in γH2AX phosphorylation, similar to the other cell line. The presence of DNA-PK inhibitors strongly affected the γH2AX assay for MDA-MB-231. When incubated with PIK-75 inhibitor, the level of γH2AX phosphorylation was slightly increased by the presence of doxorubicin, while the combination of doxorubicin and CC-115 caused a slight decrease in the γH2AX phosphorylation.

In MCF-7, the cell-cycle profile appears relatively stable across treatments (Figure 6). The control has a large S-phase fraction and a small G2/M fraction, and neither DNA-PK inhibitors or doxorubicin seem to produce a dramatic shift toward G2/M. This trend is available for the inhibitor–doxorubicin combinations as well. This suggests that, at the analyzed time point, MCF-7 does not undergo a strong checkpoint-mediated cell-cycle arrest after these treatments. That fits reasonably well with the viability data, where MCF-7 showed a more resistant and less dose-responsive phenotype. If γH2AX positivity is present but not accompanied by a major G2/M accumulation, it could indicate that MCF-

 doi:10.20944/preprints202605.0803.v1

7 tolerates or is still able to repair the damage without being forced into arrest, possibly through the known retained HR-mediated repair capacity.

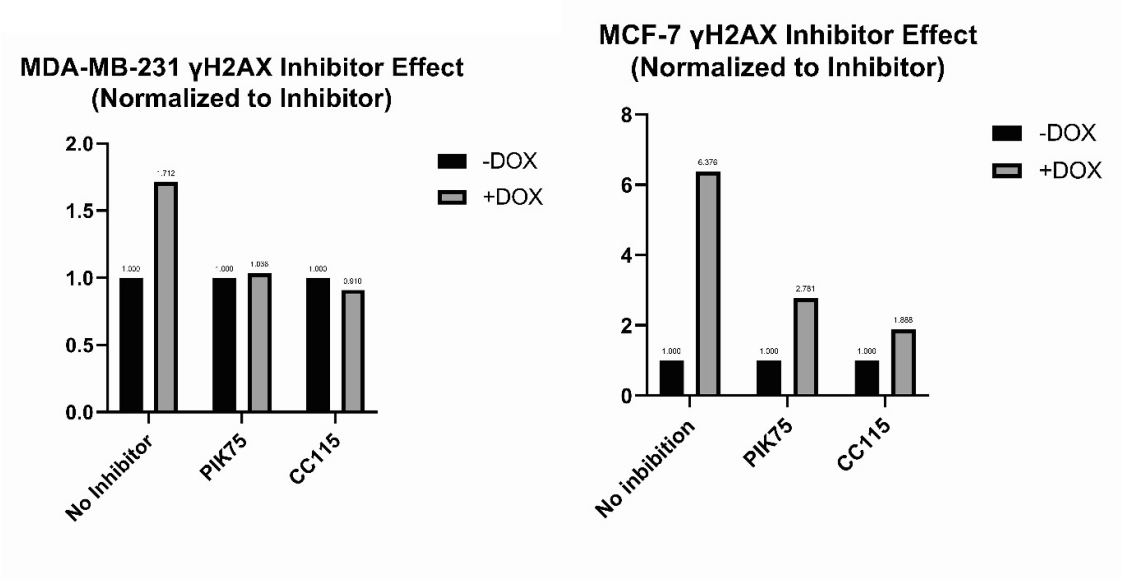

(a) (b)

Figure 5. γH2AX results: (a) γH2AX analysis of MDA-MB-231 cell line following incubation with PIK-75, CC-115 and doxorubicin; (b) γH2AX analysis of MCF-7 cell line following incubation with PIK-75, CC-115 and doxorubicin. Results are normalized their respective DNA-PK inhibitors.

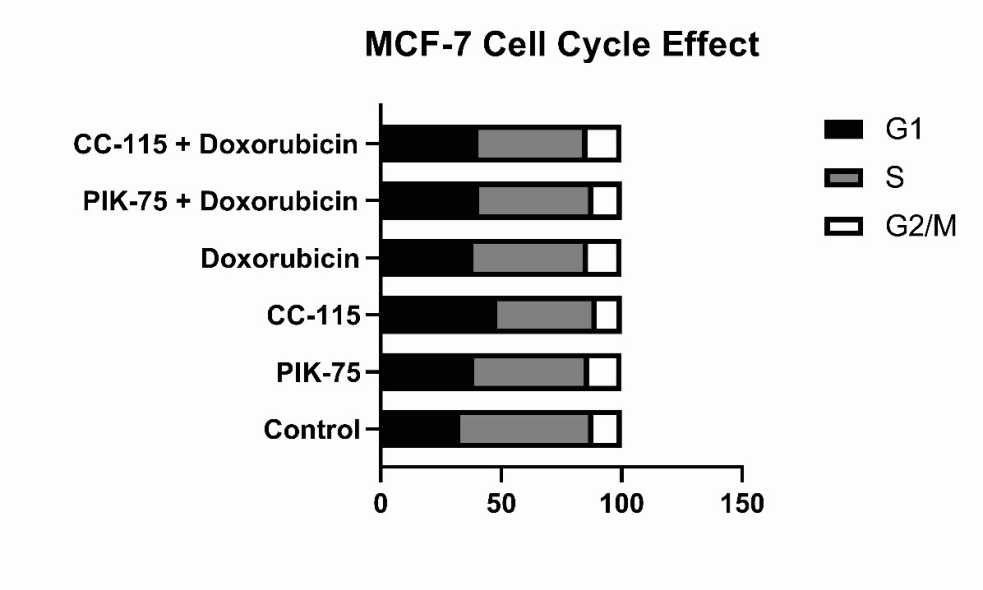

Figure 6. Cell-cycle distribution for MCF-7; The results are normalized to the total number of detected cells.

In MDA-MB-231, the cell-cycle control distribution (Figure 7) already shows a larger G2/M compartment than MCF-7, trend that is consistent across the treated groups. However, the treatment-induced changes are modest, doxorubicin alone and in combination with the inhibitors do not seem to produce clear additional G2/M accumulation compared to the control. This is interesting due to MDA-MB-231 viability data showing a much stronger delayed cytotoxicity, especially at 72 h with [^{64}Cu]$CuCl_2$ combinations. Together, these results suggest that the loss of viability in MDA-MB-231 may not be explained simply by a massive early cell-cycle arrest, but rather by the accumulation of

 doi:10.20944/preprints202605.0803.v1

unrepaired or misrepaired DNA lesions that later could be translated into apoptotic death, mitotic catastrophe, or loss of proliferative capacity.

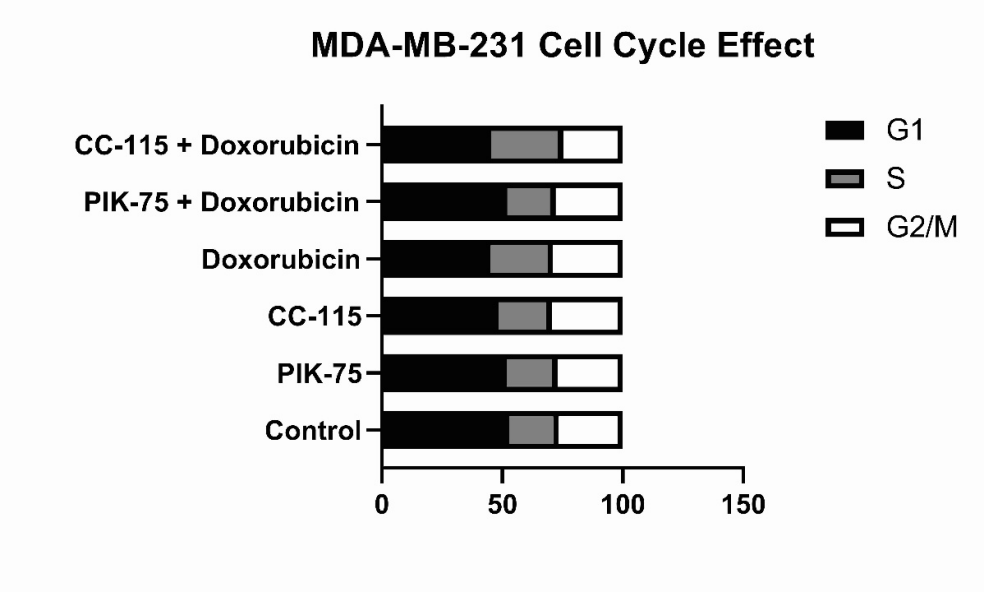

Figure 7. Cell-cycle distribution for MDA-MB-231; The results are normalized to the total number of detected cells.

3. Discussion

Across the 24h viability data, the response pattern is clearly cell-line dependent. MDA-MB-231 shows a more coherent concentration-related response to DNA-PK inhibition, especially when the inhibitors are combined with DNA-damaging treatments, whereas MCF-7 displays a flatter and more heterogeneous profile, with broader overlap between error bars and less consistent dose-dependent inhibition. This is biologically plausible if MDA-MB-231 is treated as the more NHEJ-reliant model, thus blocking DNA-PK should compromise the key DSB-repair route; published data also support that MDA-MB-231 can show low HR capacity and sensitivity to DNA-PK inhibition in the context of repair defects [32]. DNA-PK is central to NHEJ-mediated DSB repair, and its inhibition is expected to increase vulnerability to DSB-inducing agents.

The [^{64}Cu]$CuCl_2$ combination therapy suggests a stronger radiosensitizing effect in MDA-MB-231 than in MCF-7. In MDA-MB-231, [^{64}Cu]$CuCl_2$ alone maintains viability around the ~70–75% range, while several inhibitor + [^{64}Cu]$CuCl_2$ conditions reduce viability further, indicating that DNA-PK inhibition may impair the repair of radiation-induced DNA damage. This is consistent with the therapeutic rationale of [^{64}Cu]$CuCl_2$, which combines β^- and Auger electron emissions and has been shown to induce changes in viability, DNA damage, oxidative stress, and stress-response pathways in cancer cells [30]. In contrast, for MCF-7, the inhibitor + [^{64}Cu]$CuCl_2$ combinations do not consistently reduce viability below [^{64}Cu]$CuCl_2$ in monotherapy; in several conditions, viability is actually higher than with radiocopper monotherapy. This suggests that, at 24 h, MCF-7 may compensate more efficiently through HR or other DDR mechanisms, making Cu-64 radiosensitization by DNA-PK inhibition weaker or more inhibitor-specific.

In this stage, the doxorubicin combinations show the clearest potentiation, particularly in MDA-MB-231, where viability is reduced below the doxorubicin-only control for most inhibitor conditions. This supports a synergistic or at least additive interaction between DNA-PK inhibition and doxorubicin-induced genotoxic stress. The effect is also visible in MCF-7, especially for M3814 and some CC-115 conditions, although the magnitude is less uniform than in MDA-MB-231. Mechanistically, this fits well with the known role of DNA-PK inhibitors as enhancers of radiation- and pharmacological-induced DNA damage; preclinical studies with selective DNA-PK inhibition have shown potentiation of both ionizing radiation and doxorubicin effects [28]. However, from

 doi:10.20944/preprints202605.0803.v1

viability data alone, the synergetic effect should ideally be confirmed quantitatively using further analyses.

Regarding the inhibitors, M3814 appears to imprint one of the strongest inhibitory effects in its higher concentrations, thus there is a big and yet unelucidated plateau-like structure for the immediate smaller concentrations. In the future, we should investigate concentrations that lie in between C1 and C2, to get a clearer idea of the dose-effect curve. CC-115 may produce a broader effect due to its cumulative blockade of both DNA-PK and mTOR, meaning its cytotoxicity may reflect simultaneous impairment of DSB repair and pro-survival/growth signaling. This may explain why it performs well in some doxorubicin combinations but less uniformly with [^{64}Cu]$CuCl_2$. PIK-75, as a less selective DNA-PK/PI3K-targeting compound, is harder to interpret because part of its effect may come from PI3K pathway inhibition rather than DNA-PK blockade alone. Overall, the data support the hypothesis that DNA-PK inhibition preferentially sensitizes the NHEJ-reliant MDA-MB-231 model, especially to doxorubicin and radiation-induced damage, while MCF-7 shows a more resistant phenotype, likely due to retained HR capacity and compensatory DDR activity.

Time-course analysis revealed that the cytotoxic interaction between DNA-PK inhibition and [^{64}Cu]$CuCl_2$ is delayed and becomes markedly more significant at 72 h, particularly in the NHEJ-reliant MDA-MB-231 cell line. While both MCF-7 and MDA-MB-231 maintained relatively high viability at 24–48 h, MDA-MB-231 underwent a profound loss of viability by 72 h, supporting the hypothesis that DNA-PK inhibition compromises the repair of radiation-induced DNA damage in NHEJ reliant models. In contrast, the more HR-competent MCF-7 model showed only partial delayed sensitivity, suggesting compensatory DNA repair capacity or a higher threshold for radiation-induced lethality.

The marked reduction in viability observed at 72 h is consistent with the delayed biological manifestation of unresolved DNA damage, and a difference must be made between this and the fast kinetics of DSB repair. Since canonical the innate DSB repair mechanisms generally occur within 1-2 hours, for NHEJ-mediated repair, or more than 8 hours, for the HR-mediated mechanism [33], persistent damage beyond 24 h is commonly interpreted as residual or complex lesions that are difficult to repair. It was shown that retention of γH2AX foci 24 h after DNA-damaging treatment closely correlated with the loss of clonogenic survival, and cells retaining RAD51 foci 12-24 h after irradiation were likely to die after [34,35]. Multiple studies highlight that apoptotic DNA fragmentation becomes observable from 48 h onward, with clear apoptotic biological effects at 72 and even 96 h [36,37]. Additionally, DNA-PK blockade was shown to prolong this window, where the return to baseline for radiation-induced γH2AX/53BP1/pATM foci is around 6 hours, but when DNA-PK inhibition is also used in combination with radiation induced DNA damage, these foci persisted at least until 72 h, together with micronuclei and prolonged G2/M arrest [28]. The significant 72 h viability collapse in MDA-MB-231 therefore supports the hypothesis that DNA-PK inhibition compromises the repair of [^{64}Cu]$CuCl_2$-induced DNA damage, leading in the end to delayed apoptotic or mitotic cell death.

The curious results of γH2AX assay on the MDA-MB-231 cell line could be caused by the interaction between the DNA-PK inhibitors and the phosphorylation of γH2AX foci. The method detects rapid phosphorylation in the histone H2AX's surrounding molecules at serine-139 by PI3K-like kinases as a response to DSBs. The interference of the DNA-PK inhibitors with the activity of those kinases could be more prominent in the case of a NHEJ dependent cells like MDA-MB-231, compared to the MCF-7.

Previous studies have indicated that the presence of DNA-PK inhibitors caused a decrease of γH2AX foci following γ irradiation of RIC1 cells, with no other significant effects on the cells [38,39]. We noticed a similar interaction in the case of the MDA-MB-231 cells incubated with CC-115 inhibitor, with and without doxorubicin, inhibitor's presence causing a slight decrease in the γH2AX following exposure to the DNA damaging compound. Thus, future experiments will focus on overcoming the barrier DNA-PK inhibitors pose for the γH2AX assay, and analyze DNA damage by other methods, such as comet assay [40,41].

 doi:10.20944/preprints202605.0803.v1

These preliminary findings show a clear difference between the effects DNA-PK inhibition had on two breast carcinoma cell lines, based on their difference in NHEJ dependency and further offers a rational path to enhance radiotherapeutic efficacy by exploiting tumor's genotypic vulnerabilities.

Considering current results, further studies will focus on the second and third concentration of PIK-75 and CC-115 inhibitors for their radiosensitizing potential, creating the framework for future *in-vivo* characterization, looking for a better description of their impact in cellular sensitivity to genotoxic stress induced synergistically by DNA-damaging compounds and already established treatment options, especially radiotherapeutic choices.

4. Materials and Methods

4.1. DNA-PK Inhibitors

The inhibitors used in this study are PIK-75, M3814 and CC-115, obtained from Selleckchem Cat. No. S1205, Cat. No. S8586, respectively Cat. No. S7891. Stock solutions were prepared using dimethyl sulfoxide (DMSO), final concentrations used in the study were obtain through dilution with phosphate buffer solution (PBS).

4.2. Cell Cultures

Two cell lines were used, MDA-MB-231 and MCF-7. MDA-MB-231 cells were cultivated in RPMI culture media supplemented with 10% fetal bovine serum (FBS) and 1% antibiotic solution, while MCF-7 cells were cultivated in DMEM culture media with 10% fetal bovine serum (FBS), 1% antibiotic solution and non-essential amino acids.

Cells samples were prepared 24h before experiments to ensure adherence.

4.3. Incubation Experiments

Cells samples were incubated with 4 different concentrations of DNA-PK inhibitors, one hour before the DNA damaging stress factor were introduced (doxorubicin, copper-64, to ensure their presence in the cells. Copper-64 solution were in the form of $[^{64}Cu]CuCl_2$ solution, obtained and used as in previous experiments [30]. The concentration used for each inhibitor is presented in Table 1. Maximum volume used for DNA-PK inhibitor solution were up to 10% of samples culture media. For [64Cu]CuCl2 solution, a 20 MBq/ml concentration was used.

Table 1. DNA-PK concetration.

	PIK-75	**M3814**	**CC-115**
C1	1 μM	10 μM	25 μM
C2	0.5 μM	1 μM	5 μM
C3	0.1 μM	0.1 μM	0.5 μM
C4	0.01 μM	0.01 μM	0.05 μM

4.4. Viability

Cell viability was investigated using a MTS assay kit CellTiter 96® AQueous One Solution Cell Proliferation Assay kit (Promega Corporation, Madison, WI, US), using the protocol recommended by the manufacturer. The DNA-PK inhibitors effect on cell viability was tested at 24h, 48h and 72h following exposure to DNA damaging factors. At each experimental time, MTS reactive was added to the culture media, incubation for 1h followed by reading the optic density (OD) at 490 nm. Results were expressed as percentage of control cells (untreated cells) viability ±standard error of the mean.

4.5. γH2AX

Genotoxicity was investigated usig the γH2AX method. Following DNA-PK inhibitor incubation and exposure to DNA damaging factors, samples were detached, centrifuged at 2000 rpm

 doi:10.20944/preprints202605.0803.v1

for 5 minutes, and resuspended in 1 ml cold ethanol. Celltrace Oregon Green 488 (Invitrogen Thermofisher refC34555) was used for barcoding. The barcoded cells sample (cells treated with doxorubicin) where incubated for 30 minutes with 1 ml PBS with Celltrace Oregon Green 488 in the dark, tapping each 5-10 minutes to keep the cells resuspended. Sample cells were resuspended with 10 ml PBS with 2% FBS, centrifuged at 2000 rpm for 5 minutes, then resuspended in 6 ml PBS with 2% FBS. Equal amount of barcoded cells samples were added to each test sample cells tube, followed by centrifuged at 2000 rpm for 5 minutes, then resuspension in 50 µl of detergent buffer with 4% (w/v) nonfat milk for 5 minutes to block nonspecific binding. 50 µl of detergent buffer with 4% (w/v) nonfat milk containing 0.125 µg of mouse-antihuman H2AX (Ser139) antibody labeled with eFluor 660 (Invitrogen Thermofisher Catalog # 50-9865-42) were added to the cell samples for 1 h incubation at room temperature. 10 ml PBS with 2% FBS were added to the samples, followed by centrifuge at 2000 rpm for 5 minutes, and resuspension in 200 µl Hoechst 33258 solution. Samples were analyzed at CytoFLEX Flow Cytometer. Results were normalized to untreated cells without the mouse-antihuman H2AX (Ser139) antibody labeling.

5. Conclusions

Our preliminary findings outlines a difference between the effects of DNA-PK inhibitors on two cell lines of breast carcinoma, based on the difference in cellular dependence on the NHEJ pathway to respond and repair DSBs. This NHEJ dependency is a prime target for developing genotypic specific therapeutic approaches in combination with chemotherapy and radiotherapy.

Future experiments will focus on the second and third concentrations of inhibitors, in order to better analyze and characterize their interactions with the cells, and the cumulative effects when used in combinations with DSBs inducing agents.

Author Contributions: Conceptualization and design: D.A.N., R.M.Ș., D.N. and D.D., Literature search, data collection, data curation, interpretation, and analysis: D.A.N., R.M.Ș. and D.N., drafting and writing the manuscript versions: D.A.N. and R.M.Ș.; revised the manuscript and finally approved: D.N., R.M.Ș. and D.N. All authors have read and agreed to the published version of the manuscript. All authors have read and agreed to the published version of the manuscript.

Funding: This work was supported by the Doctoral Program (D.A.N.) and "Publish not Perish 2026" Program of the "Carol Davila" University of Medicine and Pharmacy, Bucharest.

Institutional Review Board Statement:

Informed Consent Statement:

Data Availability Statement:

Acknowledgments: The authors would like to acknowledge the help of our colleague Mihaela Temelie at DFVM department at IFIN-HH and Cosmin Trif at IBAR for their experimental and logistical support with chemicals and instruments.

Conflicts of Interest: The authors declare no conflicts of interest.

Abbreviations

The following abbreviations are used in this manuscript:

DSB	Double-strand break
NHEJ	Non-homologous end joining
HR	Homologous Recombination
DNA-PK	DNA-dependent protein kinase
SCLC	Small-cell lung cancer
AML	Acute myeloid leukemia
IR	Ionizing Radiation

 doi:10.20944/preprints202605.0803.v1

BBB	Blood-brain barrier
PSA	Prostate-specific antigen
DMSO	Dimetyl sulfoxide
PBS	Phosphate buffer solution
FBS	Fetal bovine serum
OD	Optic density

References

1. Lieber, M.R. The Mechanism of Double-Strand DNA Break Repair by the Nonhomologous DNA End-Joining Pathway. *Annu. Rev. Biochem.* **2010**, *79*, 181–211, doi:10.1146/annurev.biochem.052308.093131.
2. Shibata, A.; Conrad, S.; Birraux, J.; Geuting, V.; Barton, O.; Ismail, A.; Kakarougkas, A.; Meek, K.; Taucher-Scholz, G.; Löbrich, M.; et al. Factors Determining DNA Double-strand Break Repair Pathway Choice in G2 Phase. *EMBO J.* **2011**, *30*, 1079–1092, doi:10.1038/emboj.2011.27.
3. Symington, L.S.; Gautier, J. Double-Strand Break End Resection and Repair Pathway Choice. *Annu. Rev. Genet.* **2011**, *45*, 247–271, doi:10.1146/annurev-genet-110410-132435.
4. Doig, K.D.; Fellowes, A.P.; Fox, S.B. Homologous Recombination Repair Deficiency: An Overview for Pathologists. *Mod. Pathol.* **2023**, *36*, doi:10.1016/j.modpat.2022.100049.
5. Watanabe, G.; Lieber, M.R. Dynamics of the Artemis and DNA-PKcs Complex in the Repair of Double-Strand Breaks. *J. Mol. Biol.* **2022**, *434*, 167858, doi:10.1016/j.jmb.2022.167858.
6. O'Driscoll, M.; Jeggo, P.A. The Role of Double-Strand Break Repair - Insights from Human Genetics. *Nat. Rev. Genet.* **2006**, *7*, 45–54, doi:10.1038/nrg1746.
7. Frit, P.; Amin, H.; Zahid, S.; Barboule, N.; Hall, C.; Matharu, G.; Hardwick, S.W.; Chauvat, J.; Britton, S.; Chirgadze, D.Y.; et al. Structural and Functional Insights into the Interaction between Ku70/80 and Pol X Family Polymerases in NHEJ. *Nat. Commun.* **2025**, *16*, 4208, doi:10.1038/s41467-025-59133-2.
8. Xing, J.; Wu, X.; Vaporciyan, A.A.; Spitz, M.R.; Gu, J. Prognostic Significance of Ataxia-Telangiectasia Mutated, DNA-Dependent Protein Kinase Catalytic Subunit, and Ku Heterodimeric Regulatory Complex 86-kD Subunit Expression in Patients with Nonsmall Cell Lung Cancer. *Cancer* **2008**, *112*, 2756–2764, doi:10.1002/cncr.23533.
9. Hsu, F.-M.; Zhang, S.; Chen, B.P.C. Role of DNA-Dependent Protein Kinase Catalytic Subunit in Cancer Development and Treatment. *Transl. Cancer Res.* **2012**, *1*, doi:10.3978/j.issn.2218-676X.2012.04.01.
10. Ohuchi, K.; Saga, R.; Hasegawa, K.; Tsuruga, E.; Hosokawa, Y.; Fukumoto, M.; Okumura, K. DNA-PKcs Phosphorylation Specific Inhibitor, NU7441, Enhances the Radiosensitivity of Clinically Relevant Radioresistant Oral Squamous Cell Carcinoma Cells. *Biomed. Rep.* **2023**, *18*, 1–8, doi:10.3892/br.2023.1610.
11. Baumann, M.; Krause, M.; Overgaard, J.; Debus, J.; Bentzen, S.M.; Daartz, J.; Richter, C.; Zips, D.; Bortfeld, T. Radiation Oncology in the Era of Precision Medicine. *Nat. Rev. Cancer* **2016**, *16*, 234–249, doi:10.1038/nrc.2016.18.
12. Beucher, A.; Birraux, J.; Tchouandong, L.; Barton, O.; Shibata, A.; Conrad, S.; Goodarzi, A.A.; Krempler, A.; Jeggo, P.A.; Löbrich, M. ATM and Artemis Promote Homologous Recombination of Radiation-induced DNA Double-strand Breaks in G2. *EMBO J.* **2009**, *28*, 3413–3427, doi:10.1038/emboj.2009.276.
13. Huang, S.; Liu, Y.; Chen, Z.; Wang, M.; Jiang, V.C. PIK-75 Overcomes Venetoclax Resistance via Blocking PI3K-AKT Signaling and MCL-1 Expression in Mantle Cell Lymphoma. *Am. J. Cancer Res.* **2022**, *12*, 1102–1115.
14. Samuels, M.; Falkenius, J.; Bar-Ad, V.; Dunst, J.; Triest, B. van; Yachnin, J.; Rodriguez-Gutierrez, A.; Kuipers, M.; You, X.; Sarholz, B.; et al. A Phase 1 Study of the DNA-PK Inhibitor Peposertib in Combination With Radiation Therapy With or Without Cisplatin in Patients With Advanced Head and Neck Tumors. *Int. J. Radiat. Oncol. Biol. Phys.* **2024**, *118*, 743–756, doi:10.1016/j.ijrobp.2023.09.024.
15. Zheng, Z.; Amran, S.I.; Thompson, P.E.; Jennings, I.G. Isoform-Selective Inhibition of Phosphoinositide 3-Kinase: Identification of a New Region of Nonconserved Amino Acids Critical for P110α Inhibition. *Mol. Pharmacol.* **2011**, *80*, 657–664, doi:10.1124/mol.111.072546.
16. Rink, J.S.; Lin, A.Y.; Calvert, A.E.; Kwon, D.; Moxley, A.; Henrich, S.E.; Mohammadlou, A.; Zhang, X.H.; Wu, X.; Querfeld, C.; et al. Encapsulation and Delivery of the Kinase Inhibitor PIK-75 by Organic Core

 doi:10.20944/preprints202605.0803.v1

High-Density Lipoprotein-Like Nanoparticles Targeting Scavenger Receptor Class B Type 1. *ACS Appl. Mater. Interfaces* **2025**, *17*, 363–373, doi:10.1021/acsami.4c15472.

17. Moir, L.M.; Trian, T.; Ge, Q.; Shepherd, P.R.; Burgess, J.K.; Oliver, B.G.G.; Black, J.L. Phosphatidylinositol 3-Kinase Isoform-Specific Effects in Airway Mesenchymal Cell Function. *J. Pharmacol. Exp. Ther.* **2011**, *337*, 557–566, doi:10.1124/jpet.110.173583.
18. Wojtalla, A.; Fischer, B.; Kotelevets, N.; Mauri, F.A.; Sobek, J.; Rehrauer, H.; Wotzkow, C.; Tschan, M.P.; Seckl, M.J.; Zangemeister-Wittke, U.; et al. Targeting the Phosphoinositide 3-Kinase P110-α Isoform Impairs Cell Proliferation, Survival, and Tumor Growth in Small Cell Lung Cancer. *Clin. Cancer Res.* **2013**, *19*, 96–105, doi:10.1158/1078-0432.CCR-12-1138.
19. Guerreiro, A.S.; Fattet, S.; Fischer, B.; Shalaby, T.; Jackson, S.P.; Schoenwaelder, S.M.; Grotzer, M.A.; Delattre, O.; Arcaro, A. Targeting the PI3K P110α Isoform Inhibits Medulloblastoma Proliferation, Chemoresistance, and Migration. *Clin. Cancer Res.* **2008**, *14*, 6761–6769, doi:10.1158/1078-0432.CCR-08-0385.
20. Vergez, F.; Sarry, J.-E.; Gallay, N.; Fialin, C.; Scotland, S.; Demur, C.; Shepherd, P.; Danet-Desnoyer, G.; Kruczynski, A.; Payrastre, B.; et al. Anti-Leukemic Activity of PIK-75, a PI3-Kinase P110α Selective Inhibitor, In Acute Myeloid Leukemia. *Blood* **2010**, *116*, 659, doi:10.1182/blood.V116.21.659.659.
21. Cheng, C.K.; Gustafson, W.C.; Charron, E.; Houseman, B.T.; Zunder, E.; Goga, A.; Gray, N.S.; Pollok, B.; Oakes, S.A.; James, C.D.; et al. Dual Blockade of Lipid and Cyclin-Dependent Kinases Induces Synthetic Lethality in Malignant Glioma. *Proc. Natl. Acad. Sci.* **2012**, *109*, 12722–12727, doi:10.1073/pnas.1202492109.
22. Smirnova, T.; Zhou, Z.N.; Flinn, R.J.; Wyckoff, J.; Boimel, P.J.; Pozzuto, M.; Coniglio, S.J.; Backer, J.M.; Bresnick, A.R.; Condeelis, J.S.; et al. Phosphoinositide 3-Kinase Signaling Is Critical for ErbB3-Driven Breast Cancer Cell Motility and Metastasis. *Oncogene* **2012**, *31*, 706–715, doi:10.1038/onc.2011.275.
23. Zenke, F.T.; Zimmermann, A.; Sirrenberg, C.; Dahmen, H.; Kirkin, V.; Pehl, U.; Grombacher, T.; Wilm, C.; Fuchss, T.; Amendt, C.; et al. Pharmacologic Inhibitor of DNA-PK, M3814, Potentiates Radiotherapy and Regresses Human Tumors in Mouse Models. *Mol. Cancer Ther.* **2020**, *19*, 1091–1101, doi:10.1158/1535-7163.MCT-19-0734.
24. Mortensen, D.S.; Perrin-Ninkovic, S.M.; Shevlin, G.; Elsner, J.; Zhao, J.; Whitefield, B.; Tehrani, L.; Sapienza, J.; Riggs, J.R.; Parnes, J.S.; et al. Optimization of a Series of Triazole Containing Mammalian Target of Rapamycin (mTOR) Kinase Inhibitors and the Discovery of CC-115. *J. Med. Chem.* **2015**, *58*, 5599–5608, doi:10.1021/acs.jmedchem.5b00627.
25. Thijssen, R.; Ter Burg, J.; Garrick, B.; van Bochove, G.G.W.; Brown, J.R.; Fernandes, S.M.; Rodríguez, M.S.; Michot, J.-M.; Hallek, M.; Eichhorst, B.; et al. Dual TORK/DNA-PK Inhibition Blocks Critical Signaling Pathways in Chronic Lymphocytic Leukemia. *Blood* **2016**, *128*, 574–583, doi:10.1182/blood-2016-02-700328.
26. Munster, P.; Mita, M.; Mahipal, A.; Nemunaitis, J.; Massard, C.; Mikkelsen, T.; Cruz, C.; Paz-Ares, L.; Hidalgo, M.; Rathkopf, D.; et al. <p>First-In-Human Phase I Study Of A Dual mTOR Kinase And DNA-PK Inhibitor (CC-115) In Advanced Malignancy</P>. *Cancer Manag. Res.* **2019**, *11*, 10463–10476, doi:10.2147/CMAR.S208720.
27. Zhao, J.L.; Antonarakis, E.S.; Cheng, H.; George, D.J.; Aggarwal, R.R.; Abida, W.; Decker, B.; Smart-Curley, T.; Schonhoft, J.; Anderson, A.; et al. 598P A Phase Ib Study of Enzalutamide (Enza) plus CC-115 in Men with Metastatic Castration-Resistant Prostate Cancer (mCRPC). *Ann. Oncol.* **2021**, *32*, S643–S644, doi:10.1016/j.annonc.2021.08.1111.
28. Fok, J.H.L.; Ramos-Montoya, A.; Vazquez-Chantada, M.; Wijnhoven, P.W.G.; Follia, V.; James, N.; Farrington, P.M.; Karmokar, A.; Willis, S.E.; Cairns, J.; et al. AZD7648 Is a Potent and Selective DNA-PK Inhibitor That Enhances Radiation, Chemotherapy and Olaparib Activity. *Nat. Commun.* **2019**, *10*, 5065, doi:10.1038/s41467-019-12836-9.
29. Niculae, D.; Dusman, R.; Leonte, R.A.; Chilug, L.E.; Dragoi, C.M.; Nicolae, A.; Serban, R.M.; Niculae, D.A.; Dumitrescu, I.B.; Draganescu, D. Biological Pathways as Substantiation of the Use of Copper Radioisotopes in Cancer Theranostics. *Front. Phys.* **2021**, *8*, doi:10.3389/fphy.2020.568296.
30. Serban, R.M.; Niculae, D.; Manda, G.; Neagoe, I.; Dobre, M.; Niculae, D.A.; Temelie, M.; Mustăciosu, C.; Leonte, R.A.; Chilug, L.E.; et al. Modifications in Cellular Viability, DNA Damage and Stress Responses Inflicted in Cancer Cells by Copper-64 Ions. *Front. Med.* **2023**, *10*, doi:10.3389/fmed.2023.1197846.

 doi:10.20944/preprints202605.0803.v1

31. Ciszewski, W.M.; Tavecchio, M.; Dastych, J.; Curtin, N.J. DNA-PK Inhibition by NU7441 Sensitizes Breast Cancer Cells to Ionizing Radiation and Doxorubicin. *Breast Cancer Res. Treat.* **2014**, *143*, 47–55, doi:10.1007/s10549-013-2785-6.
32. Lee, K.J.; Mann, E.; Wright, G.; Piett, C.G.; Nagel, Z.D.; Gassman, N.R. Exploiting DNA Repair Defects in Triple Negative Breast Cancer to Improve Cell Killing. *Ther. Adv. Med. Oncol.* **2020**, *12*, 1758835920958354, doi:10.1177/1758835920958354.
33. Penninckx, S.; Pariset, E.; Cekanaviciute, E.; Costes, S.V. Quantification of Radiation-Induced DNA Double Strand Break Repair Foci to Evaluate and Predict Biological Responses to Ionizing Radiation. *NAR Cancer* **2021**, *3*, zcab046, doi:10.1093/narcan/zcab046.
34. Banáth, J.P.; Klokov, D.; MacPhail, S.H.; Banuelos, C.A.; Olive, P.L. Residual γH2AX Foci as an Indication of Lethal DNA Lesions. *BMC Cancer* **2010**, *10*, 4, doi:10.1186/1471-2407-10-4.
35. Takano, S.; Shibamoto, Y.; Wang, Z.; Kondo, T.; Hashimoto, S.; Kawai, T.; Hiwatashi, A. Optimal Timing of a γH2AX Analysis to Predict Cellular Lethal Damage in Cultured Tumor Cell Lines after Exposure to Diagnostic and Therapeutic Radiation Doses. *J. Radiat. Res. (Tokyo)* **2023**, *64*, 317–327, doi:10.1093/jrr/rrac096.
36. Ghardi, M.; Moreels, M.; Chatelain, B.; Chatelain, C.; Baatout, S. Radiation-Induced Double Strand Breaks and Subsequent Apoptotic DNA Fragmentation in Human Peripheral Blood Mononuclear Cells. *Int. J. Mol. Med.* **2012**, *29*, 769–780, doi:10.3892/ijmm.2012.907.
37. Brunner, S.; Varga, D.; Bozó, R.; Polanek, R.; Tőkés, T.; Szabó, E.R.; Molnár, R.; Gémes, N.; Szebeni, G.J.; Puskás, L.G.; et al. Analysis of Ionizing Radiation Induced DNA Damage by Superresolution dSTORM Microscopy. *Pathol. Oncol. Res.* **2021**, *27*, 1609971, doi:10.3389/pore.2021.1609971.
38. Urushihara, Y.; Kobayashi, J.; Matsumoto, Y.; Komatsu, K.; Oda, S.; Mitani, H. DNA-PK Inhibition Causes a Low Level of H2AX Phosphorylation and Homologous Recombination Repair in Medaka (*Oryzias Latipes*) Cells. *Biochem. Biophys. Res. Commun.* **2012**, *429*, 131–136, doi:10.1016/j.bbrc.2012.10.128.
39. Hain, K.O.; Colin, D.J.; Rastogi, S.; Allan, L.A.; Clarke, P.R. Prolonged Mitotic Arrest Induces a Caspase-Dependent DNA Damage Response at Telomeres That Determines Cell Survival. *Sci. Rep.* **2016**, *6*, 26766, doi:10.1038/srep26766.
40. Jaiswal, M.; Anuradha, G.; Rajeswari, N.; Ahuja, Y.R. Single Cell Gel Electrophoresis Assay (Comet Assay): Its Importance in Human Biology. *Int. J. Anthropol.* **1995**, *10*, 177–181, doi:10.1007/BF02447874.
41. Olive, P.L.; Banáth, J.P. The Comet Assay: A Method to Measure DNA Damage in Individual Cells. *Nat. Protoc.* **2006**, *1*, 23–29, doi:10.1038/nprot.2006.5.